Transverse X-Ray Coherence in Nuclear Scattering of Synchrotron Radiation

A. Q. R. Baron, A. I. Chumakov, H. F. Grünsteudel, H. Grünsteudel,* L. Niesen,† and R. Rüffer
European Synchrotron Radiation Facility (ESRF), BP 220, F-38043 Grenoble Cedex, France
(Received 17 July 1996)

The time response of nuclei excited by pulsed synchrotron radiation is affected by correlations in the nuclear response transverse to the beam direction. The coherent addition of the radiation scattered by nuclei having a distribution of Doppler shifts accelerates the decay in the forward scattering from a rotating foil of ^{57}Fe stainless steel. A model based on Huygens's construction shows good agreement with the data, allowing estimation of the source size or transverse coherence length. Implications for spectroscopic experiments using nuclear forward scattering are discussed. [S0031-9007(96)01697-3]

PACS numbers: 76.80.+y, 42.25.Hz, 78.70.Ck

Conclusions about microscopic properties are frequently drawn from measurements of macroscopic samples. This is true for most experiments using x-ray probes since x-ray sources are generally too weak (and the relevant cross sections too small) to directly investigate microscopic samples. It is then necessary to properly relate the macroscopic measurement to the microscopic response. For this purpose, one identifies the limits of incoherent and coherent scattering [1]. Most x-ray spectroscopic measurements (e.g., XAFS, x-ray fluorescence) measure incoherent scattering processes which are essentially local. Structural measurements (e.g., diffraction), in contrast, typically investigate coherent scattering from extended portions of the sample.

This paper explores coherence in a relatively new type of spectroscopy: nuclear forward scattering (NFS) of synchrotron radiation [2,3]. NFS experiments might be considered the time-domain analog of conventional frequency-domain Mössbauer transmission experiments. They examine the time response of nuclei excited by a pulse of synchrotron radiation, preserving the in-line source-sample-detector arrangement of the transmission experiment. However, where the transmission experiment measures the absorption of a beam passing through a sample, the NFS measures the coherently re-emitted wave field. Reviews of nuclear scattering of synchrotron radiation may be found in [4] and [5], while some aspects of coherence in such measurements are discussed in [6].

Coherence in NFS is immediately interesting and pertinent for a sample having different nuclear environments. If these environments result in different nuclear response frequencies, then coherent combination of their impulse responses will give corresponding quantum beats in the time response, while incoherent combination will not. Previous work has investigated several limits. NFS from metallic ^{57}Fe samples shows beats between the transitions to different (Zeeman split) ground states [2,3]. Similarly, two samples placed in succession, one after the other, in the x-ray beam (or in the arms of an amplitude splitting interferometer [7]) give a time response in NFS that is a coherent combination of the responses of the individual samples.

Here, as distinct from previous work, we focus on the effects of *transverse* coherence: how the responses of nuclei in a sample separated perpendicular to the beam combine in forward scattering. Interest in the effects of transverse coherence, including speckle measurements [8,9] and phase contrast microscopy [10,11] is increasing with the advent of higher brilliance x-ray sources. With nuclear scattering, one may combine a spectroscopic measurement with structural information from transverse coherence. Aside from its basic physical interest, transverse coherence is of practical importance for NFS measurements on thin samples exhibiting domain structure [12]. *A priori*, one might expect there to be two limits: a "well-mixed" sample where the response of the nuclei should be added coherently and a "well-separated" case where the responses would add incoherently. This paper investigates the border between these limits.

The essential concept for this experiment is that we introduce a uniform spatial gradient in the velocity of nuclei in a sample, resulting in a corresponding spatial gradient in the Doppler shift in their response (absorption/emission) frequencies. This gradient is carefully arranged so that all nuclei along the path of an infinitesimal cross section beam respond at the same frequency, and also so that transverse displacement of this beam will shift that frequency. Noting that the NFS time response of a moving foil is independent of its absolute velocity, the gradient introduced in this fashion will only affect the measured time response if there is a coherent addition of the scattering from transversely separated portions of the sample. In particular, the coherent addition of the scattering from nuclei with a distribution of Doppler shifts, essentially a broadening of the frequency response, is expected to result in a faster decay of the impulse response. This acceleration of the decay is the signal we look for and observe.

This work was done at the nuclear resonance beam line [13] of the European Synchrotron Radiation Facility (ESRF). The synchrotron provided short ($\sim$120 ps) pulses of x rays every 2.8 μs. The bandwidth of the 14.4 keV radiation was reduced to 3 eV using a

 0031-9007/96/77(23)/4808(4)$10.00

Si 111 monochromator and then to 6 meV using "high resolution monochromator" [13–15]. The radiation was allowed to fall onto a stainless steel (SS) foil (4.5 mg/cm^2) 95% enriched in ^{57}Fe, oriented at 45° to the beam path. The foil was mounted on a dc motor (horizontal axis perpendicular to the foil surface) run at rotation rates up to 100 Hz. An avalanche diode detector [16] measured the NFS time response (see Fig. 1). Slits limiting the vertical aperture of the system were placed immediately (10 cm) after the foil and just (4 cm) in front of the detector. The slits were measured with the x-ray beam to be 15 μm high, full width at half maximum (FWHM). They were larger than the beam size in the horizontal. With the slits in place, count rates were ~10 photons/s in the time window of about 10–150 ns after the synchrotron pulse (~10 mA storage ring current).

The NFS from the SS foil at rest is shown in Fig. 2(a). This is well fit using an exponential decay modulated by a Bessel function, as expected for the NFS from a single line nuclear response [3,17]. As the rotation rate is increased [Fig. 2(b)–2(d)], the decay becomes much faster. This demonstrates interference between transversely separated parts of the beam. In contrast, the response measured at high rotation rate, *without* slits, is indistinguishable from that measured at rest [Fig. 2(a)]. One also notes that, within statistics, the location of the Bessel minimum (at $t \sim 55$ ns) was not affected by rotation.

In order to understand these results we develop a model based on Huygens's construction. For a point source, the response observed by a pointlike detector is the integral over the secondary waves emitted by the nuclei in the sample. Taking the impulse response of the foil at rest to be $G_0(t)$, integration over the foil yields the time-dependent field amplitude at the detector

$$E(z_0, z_d, t) \propto G_0(t) \int dz_s e^{-iz_s t/A\tau_0} e^{i\varphi(z_0, z_s, z_d)} W_s(z_s) . \quad (1)$$

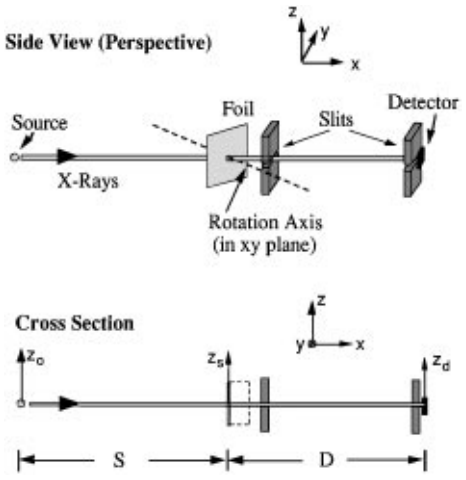

FIG. 1. Experimental setup. The perspective drawing shows the general orientation while the cross section shows quantities used in the text. The source-sample distance was $S = 41$ m. The detector was $D = 2.5$ m downstream of the sample.

z_0 is the location of the point source, z_d is the location of a point detector, and z_s is the source point of the secondary waves in the sample (see Fig. 1). $W_s(z_s)$ is the field amplitude at the sample. The first exponential accounts for the Doppler shift in the nuclear response frequency with height [18]. τ_0 is the natural lifetime of the nucleus ($\tau_0 = 141$ ns for ^{57}Fe), and A is the vertical distance necessary to shift the nuclear response frequency by one natural linewidth. One has $A = v_0/2\pi N \sin\theta$ where θ is the angle between the rotation axis and the beam direction, v_0 is the Doppler velocity corresponding to a natural linewidth, and N is the rotation frequency. Taking $v_0 = 97$ μm/sec (appropriate for the 14.4 keV resonance of ^{57}Fe) and $\theta = \pi/4$, $A[\mu\text{m}] = 22/N[\text{Hz}]$.

φ in Eq. (1) is the (relative) geometric phase associated with the different path lengths for different points of the sample. Taking S to be the distance from the source plane to the sample plane and D the distance from the sample plane to the detector (see Fig. 1), one has ($k = 2\pi/\lambda$)

$$\varphi(z_0, z_s, z_d) = -k\left(\frac{z_0}{S} + \frac{z_d}{D}\right) + \frac{k}{2}\left(\frac{1}{S} + \frac{1}{D}\right) z_s^2 . \quad (2)$$

The term linear in z_s is kept in the usual Fraunhofer limit [19]. For our experimental geometry, terms of higher order than second are negligible.

One must integrate the intensity over the finite source and detector sizes. For a detector of spatial acceptance given by W_d, and a source intensity distribution W_0, the

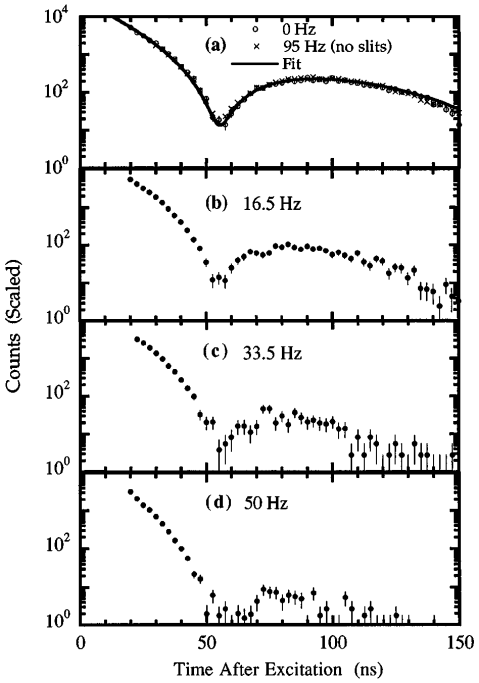

FIG. 2. Forward scattered time response for (a) the foil at rest (with slits in place) or at 95 Hz without slits. (b)–(d) show the response at higher rotation rates. (b)–(d) are normalized in the same incident rate and counting time as the response at rest in (a).

measured time response is

$$I(t) \propto \int \int dz_0 dz_d |E(z_0, z_d, t)|^2 W_0(z_0) W_d(z_d) . \quad (3)$$

Momentarily, we illustrate some of the essential concepts of this problem by considering a time-domain two slit interference pattern. If the rotating foil is masked by two small slits, having separation L, and, for simplicity, negligible height, the intensity measured by a point detector at z_d for a point source at z_0 is found from Eq. (1) by taking $W_S(z_s) = \delta(z_s + L/2) + \delta(z_s - L/2)$,

$$I(z_0, z_d, t) \propto |G_0(t)|^2 \left[1 + \cos\left(\Omega t + kL\frac{z_0}{S} + kL\frac{z_d}{D} \right) \right], \quad (4)$$

where $\Omega = L/A\tau_0$ is the frequency difference between the response at the $+L/2$ and $-L/2$ locations of the slits.

The intensity variation with detector position (for t fixed) is a two-slit spatial interference pattern with angular period λ/L. The intensity contrast is a direct indication of the coherence of the scattering from the two slits [20]. If either the source or the detector subtend angles larger than λ/L, the contrast will be reduced and the slit responses become incoherent. The same effect occurs in the time response. The two geometric terms in the cosine determine the initial phase of the temporal beat pattern, which then oscillates with frequency $\Omega/2\pi$. Large detector or source sizes lead to integration over differently phased beat patterns and incoherent superposition of responses. This qualitatively demonstrates the importance of the slit in front of the detector and small source size.

Returning to the rotating foil calculation, an analytic form for the response may be derived if all distributions are assumed to be Gaussian (where the size of the source, the beam on the sample, and the detector are given by σ_0, σ_s, and σ_d, respectively). This gives [21]

$$I(\tilde{z}_d, t > 0) \propto |G_0(t)|^2 \exp\left[-\frac{1}{2\alpha^2}\left(\frac{1}{kA}\frac{t}{\tau_0} + \frac{\tilde{z}_d}{D} \right)^2 \right]. \quad (5)$$

The quantity $\tilde{z}_d$ allows for a possible offset of the center of the detector from the direct line of the source and sample. α is the measured divergence of the radiation from the foil at rest:

$$\alpha^2 = \frac{\sigma_0^2}{S^2} + \frac{\sigma_d^2}{D^2} + \left(\frac{\sigma_s}{D} + \frac{\sigma_s}{S} \right)^2 + \frac{1}{4k^2\sigma_s^2} . \quad (6)$$

The various terms in α are identified as the effects of finite source, detector and sample sizes, and the Fraunhofer diffraction term, respectively.

The foil responds with a reduced lifetime and a shift in the time response. Both may be qualitatively explained by the two-slit example. The shift in the time response with detector position is directly analogous to the above mentioned shift in phase of the beat pattern with detector position. Here, however, only the initial part of the "beat" pattern is visible before the continuum of excited frequencies washes it out. Likewise, the observed lifetime is modified by the detector, source, and sample sizes, as one integrates over the different phasing of the response pattern. Large detectors, sources, and samples blur the interference pattern leading to measurement of an incoherent response.

The measured time responses, divided by the fit to the time response at zero rotation rate, are shown in Fig. 3. The solid lines are calculations using Eq. (3), assuming slits of 15 μm height limit the illumination of the sample and detector. In order to obtain good agreement with the data, it was necessary to assume a source size of about 290 μm FWHM ($\sigma_0 = 120$ μm). In contrast, measurements of the electron beam emittance suggest the vertical source size should be about 55 μm FWHM [22]. The difference is explained by imperfect transport of the x-ray beam from the source to the sample. In general, this could be the result of windows and filters installed on the beam line [11,23]. However, recent measurements [24] of the fringes from a boron fiber [10] are in agreement with the results measured here and show that the dominant contribution to the increase in the source size is due to the high resolution monochromator.

Figure 4 demonstrates the effect of shifting the detector out of the direct line of source and sample (i.e., to finite $\tilde{z}_d$). As expected from Eq. (5), there is a shift in the peak of the time response. This shift (and the good agreement with theory) is further confirmation of the interpretation presented here. One notes that this not a slowing down of the NFS response, which shows an accelerated decay after the peak is reached.

We define an effective coherence length L_c as the minimum transverse separation between parts of the sample necessary to ensure that their responses add incoherently. Investigation of Eqs. (5) and (6), or extension of Eq. (4), gives $L_c \sim \lambda/2\pi\alpha$. In the limit that both the detector

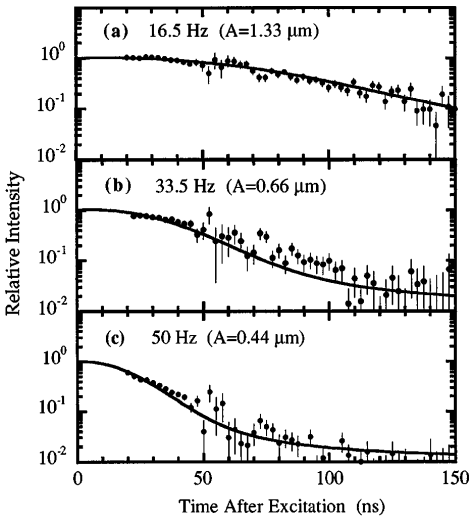

FIG. 3. Measured time responses divided by the fit to the response at rest. Solid lines are calculations based on Eq. (3). The vertical scale is the intensity relative to response of the foil at rest.

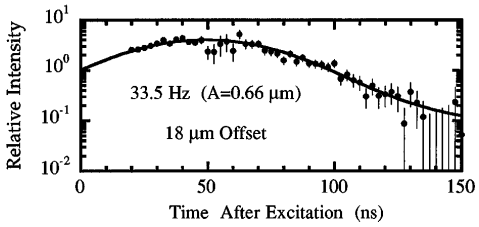

FIG. 4. Effect of moving the detector off the direct source-sample axis. The phasing of the scattered wave shifts the peak of the response to later times. Normalization as in Fig. 3.

and sample are small, this definition corresponds with the usual one (see, e.g., [20]). However, as the effects of sample and detector sizes are not negligible for most NFS measurements, we explicitly include them here. In fact, typical running conditions at ESRF (*without* the small slits used here) will be dominated by the $\sigma_d \sim 0.5$ mm detector acceptance at a distance of $D \sim 1$ m. One then expects incoherent addition of the responses for parts of the sample separated transversely by more than $L_c \sim 300$ Å. However, bulk samples exhibiting structure of this scale transverse to the x-ray beam may be expected to have similar structure parallel to the beam direction [25]. This should result in coherent combination of the various responses until the domain size begins to approach the sample thickness, in which case incoherent addition would begin to dominate.

An application of this work would be to change effective coherence length to investigate the scale of variation of the nuclear response in a sample. With the slits used here, $L_c \sim 3$ μm, but one could hope to increase this length a factor of 2 or more, by increasing the sample-detector separation or shrinking slit sizes. Removal of the detector to infinity makes this an angular resolved measurement, so one expects to see similar changes in the time response by employing a crystal analyzer after the sample [26]. Recent work shows this is the case [27], and such an analyzer might provide an easier method of investigating the sample length scales via the time response than the slits used here, which reduce the count rate. Finally, while the velocity correlation introduced in this work provides a good test case, more generally, the nuclear scattering amplitude is sensitive to hyperfine fields (magnetic dipole and electric quadrapole) and even to chemical binding (isomer shifts), so one may investigate length correlations in these quantities as well.

A. B. would like to thank P. Cloetens for discussing this work with him. We also thank the ESRF staff for helping to make experiments possible on ID18, particularly, J. Ejton and Z. Hubert. We thank E. Gerdau for the loan of the SS foil. H. G. acknowledges the support of the Deutsche Forschungsgemeinschaft.

*On leave from Medizinische Universität zu Lübeck, Institut für Physik, Ratzeburger Allee 160, D-23538 Lübeck, Germany.

†Permanent address: Nuclear Solid State Physics, Materials Science Center, University of Groningen, Nÿenborgh 4, 9747 AG Groningen, Netherlands.

[1] See, e.g., S. W. Lovesey, *Theory of Neutron Scattering from Condensed Matter*, edited by R. K. Adair *et al.*, International Series of Monographs on Physics (Clarendon Press, Oxford, 1994), Vol. 1.
[2] J. B. Hastings *et al.*, Phys. Rev. Lett. **66**, 770 (1991).
[3] U. van Bürck *et al.*, Phys. Rev. B **46**, 6207 (1992).
[4] E. Gerdau and U. van Bürck, in *Resonant Anomalous X-Ray Scattering. Theory and Applications*, edited by G. Materlik, C. J. Sparks, and K. Fischer (Elsevier, New York, 1994), pp. 589–608.
[5] G. V. Smirnov, Hyperfine Interact. **97/98**, 551 (1996).
[6] U. van Bürck and G. V. Smirnov, Hyperfine Interact. **90**, 313 (1994).
[7] K. Izumi *et al.*, Jpn. J. Appl. Phys. **34**, 4258 (1995).
[8] M. Sutton *et al.*, Nature (London) **352**, 608 (1991).
[9] S. Brauer *et al.*, Phys. Rev. Lett. **74**, 2010 (1995).
[10] A. Snigirev *et al.*, Rev. Sci. Instrum. **66**, 5486 (1995).
[11] P. Cloetens *et al.*, J. Phys. D **29**, 133 (1996).
[12] H. F. Grünsteudel *et al.*, Hyperfine Interact. C **1**, 509 (1996).
[13] R. Rüffer and A. I. Chumakov, Hyperfine Interact. **97/98**, 589 (1996).
[14] T. Ishikawa *et al.*, Rev. Sci. Instrum. **63**, 1015 (1992).
[15] T. S. Toellner, T. Mooney, S. Shastri, and E. E. Alp, in *Optics for High-Brightness Synchrotron Beamlines*, edited by J. Arthur SPIE Proceedings Vol. 1740 (SPIE-International Society for Optical Engineering, Bellingham, WA, 1992), p. 218.
[16] A. Q. R. Baron, Nucl. Instrum. Methods Phys. Res., Sect. A **353**, 665 (1994).
[17] Y. Kagan, A. M. Afanas'ev, and V. G. Kohn, J. Phys. C **12**, 615 (1979).
[18] The velocity along the direction of x-ray propagation depends only on the height above the (horizontal) plane containing the x-ray beam and the rotation axis.
[19] M. Born and E. Wolf, *Principles of Optics* (Pergamon Press, New York, 1980), pp. 382–386.
[20] L. Mandel and E. Wolf, Rev. Mod. Phys. **37**, 231 (1965).
[21] The integral over the exponential of a second order polynomial with complex coefficients may be found in I. S. Gradshteyn and I. M. Ryzhik, *Table of Integrals, Series and Products* (Academic Press, Inc., New York, 1980), p. 485, Eq. 3.923.
[22] J. M. Filhol (private communication).
[23] A. Snigirev, I. Snigireva, V. G. Kohn, and S. M. Kuznetsov, Nucl. Instrum. Methods Phys. Res., Sect. A **370**, 634 (1996).
[24] A. Snigirev, I. Snigireva, C. Raven, and M. Drakopoulos performed these measurements.
[25] Some structured samples, especially multilayers in a grazing incidence specular reflection geometry, might provide exceptions.
[26] This is similar to a small angle scattering geometry. In fact, the *angular* distribution of nuclear scattering gives information about magnetic correlation lengths in iron samples. Yu. V. Shvyd'ko *et al.*, in Phys. Rev. B (to be published).
[27] A. Q. R. Baron *et al.* (unpublished); and also R. Röhlsberger (private communication).